Transportation Engineering 3 (2021) 100040

Contents lists available at ScienceDirect

Transportation Engineering

journal homepage: www.elsevier.com/locate/treng

Studying hydraulic conductivity of asphalt concrete using a database

Shuyin Feng [a,1], Paul J. Vardanega [a,2,*], Maximilian James [b,3], Erdin Ibraim [a,4]

[a] Department of Civil Engineering, University of Bristol, Bristol BS8 1TR, UK
[b] Formerly Department of Civil Engineering, University of Bristol, Bristol BS8 1TR, UK

ARTICLE INFO

Keywords:
Hydraulic conductivity
Grading entropy
Effective particle size
Gradation parameter
Nominal maximum aggregate size

ABSTRACT

A new database called AC/k-1624 containing over 1600 measurements of saturated hydraulic conductivity of asphalt concrete has been assembled and analysed. AC/k-1624 was used to investigate the effect of the grading entropy parameters on saturated hydraulic conductivity. A new prediction model comprising both air voids and grading entropy is presented. The database analysis using different predictors of asphalt hydraulic conductivity reveals that the gradation does affect the hydraulic conductivity, but the air void level is necessary to make reasonable a-priori assessments of hydraulic conductivity for asphalt concrete. The new empirical model is shown to have a good predictive capacity for hydraulic conductivity fitting more securely at higher values with more scatter observed at lower values. The effects of test type, gradation classification and Nominal Maximum Aggregate Size (NMAS) are also studied, revealing in general relatively modest influences on the computed regression coefficients.

1. Introduction

Assessing the propensity for asphalt concrete pavement layers to allow the flow of water throughout is important for understanding pavement performance [1]. Hydraulic conductivity (k) of asphalt concrete has been the subject of sustained research efforts in recent decades [e.g., 2–14]. This paper reviews the influence of different predictors for k of asphalt concrete using a database called AC/k-1624. The database contains over 1600 measurements of k on asphalt concrete mixtures and builds upon previous database analyses of this important parameter. An early version of this database was presented in Vardanega and Waters [15] ($n = 467$) and was subsequently expanded in Vardanega et al. [16] ($n = 1318$) as well as Feng [17] ($n = 1578$). The aim of this paper is to bring together and revisit the results of the previous studies and develop a novel empirical model for asphalt concrete k that incorporates both the percentage air void ($AV\%$) level and a grading entropy parameter (a similar concept for gravels was recently proposed by O'Kelly and Nogal when discussing Feng et al. [18,19] and presented in detail in O'Kelly and Nogal [20]). In particular, this study aims to: (i) Report the details of the sources of data used to build AC/k-1624; (ii) Develop transformation models [21,22] linking measurements of saturated k to simple asphalt concrete mix parameters and determine the key predictors of asphalt concrete k; and (iii) Study the potential effects of test type, gradation type and Nominal Maximum Aggregate Size ($NMAS$) on the k of asphalt concrete.

2. Literature review

Asphalt concrete k is an important parameter to model the effects of water ingress into all parts of the pavement structure. The k of asphalt concrete is highly anisotropic [23,24] although the degree of anisotropy may be reduced at higher $AV(\%)$ levels [25] and increasing depth from the top surface [26].

2.1. Air Voids

The need for some measure of porosity (void ratio) is well documented in studies of flow through porous media in the geotechnical and pavement engineering context [14,27–31]. Zube [28] emphasised the need for the use of $AV(\%)$ as a predictor of the k of asphalt concrete. The importance of evaluating connected voids has also been demonstrated by Tarefder and Ahmad [32] and Feng et al. [33]. Detailed studies on the distribution of air voids and pore structure have also been published [34–36].

* Corresponding author.
E-mail addresses: shuyin.feng@bristol.ac.uk (S. Feng), p.j.vardanega@bristol.ac.uk (P.J. Vardanega), mj12749.2012@my.bristol.ac.uk (M. James), Erdin.Ibraim@bristol.ac.uk (E. Ibraim).
[1] PhD Student, Department of Civil Engineering, University of Bristol, Bristol, BS8 1TR, UK. [ORCID: 0000-0002-3837-6762]
[2] Senior Lecturer in Civil Engineering, Department of Civil Engineering, University of Bristol, Bristol, BS8 1TR, UK. [ORCID: 0000-0001-7177-7851]
[3] Formerly MEng student, Department of Civil Engineering, University of Bristol, Bristol, BS8 1TR, UK
[4] Associate Professor in Geomechanics, Department of Civil Engineering, University of Bristol, Bristol, BS8 1TR, UK

https://doi.org/10.1016/j.treng.2020.100040
Received 24 September 2020; Received in revised form 7 December 2020; Accepted 8 December 2020

Notation: The following notation is used in this paper (units given in brackets for those quantities with units)

A	relative base entropy;
a	a coefficient;
$AV\%$	air void percentage;
B	normalised entropy increment;
b	a coefficient;
C_i	number of elementary statistical cells in fraction i;
D_{10}	effective particle size, for which 10% of the soil is finer (length);
D_{20}	effective particle size, for which 20% of the soil is finer (length);
D_{25}	effective particle size, for which 25% of the soil is finer (length);
D_{30}	effective particle size, for which 30% of the soil is finer (length);
D_{40}	effective particle size, for which 40% of the soil is finer (length);
D_{50}	effective particle size, for which 50% of the soil is finer (length);
D_{60}	effective particle size, for which 60% of the soil is finer (length);
D_{70}	effective particle size, for which 70% of the soil is finer (length);
D_{75}	effective particle size, for which 75% of the soil is finer (length);
D_{90}	effective particle size, for which 90% of the soil is finer (length);
D_x	effective particle size;
H	entropy of a set of probabilities;
k	hydraulic conductivity (length. time^{-1});
n	number of data points;
N	number of fractions;
NV	normalised voids;
$NMAS$	nominal maximum aggregate size (length);
p	*p-value*;
p_i	probability of a system being in cell i of its phase space;
PSD	particle size distribution;
R^2	coefficient of determination;
R_p	representative pore size (length);
S	grading entropy;
S_0	base entropy;
SE	standard error;
x_i	relative frequency of fraction i;
ΔS	entropy increment.

2.2. Effective particle size

There have been many studies exploring the effects of mixture gradation on the k of asphalt concrete [2,15,37–39]. Waters [2,40] used the 'normalised air voids' (NV, which incorporates $AV(\%)$ and the D_{50}) as a predictor for k of asphalt concrete. Following this work, Vardanega and Waters [15] reported a database (n = 467) and following subsequent analysis showed that the 'representative pore size' (R_p) with D_{75} as the effective particle size was a good predictor of asphalt concrete k giving the following equation:

$$k\,(mm/s) = 0.46\left(R_p\right)^{3.7} \tag{1}$$

where:

$$R_p = 2/3 \times (AV\%/100) \times D_x \tag{2}$$

in which D_x is the effective particle size in mm (taken as D_{75}) in Vardanega and Waters [15]. Vardanega et al. [16] updated the database of Vardanega and Waters [15] (n=1318) and showed that R_p remained a good predictor of asphalt concrete k.

2.3. Grading entropy

The 'grading entropy' concept, proposed by Lőrincz in 1986 [41], describes the order (or disorder) in the particle size distribution (PSD) of the material by applying entropy theory [42]. The grading entropy framework has been used to investigate, e.g., soil particle loss [43], soil crushing [44,45], soil stability [45,46], soil texture [47] and soil permeability k [17,18,48].

The entropy of a set of probabilities p_1, …, p_n can be computed as:

$$H = -\sum p_i \log pi \tag{3}$$

where: p_i is the probability of a system being in cell i of its phase space [42].

To compute the statistical entropy of the PSD, a double statistical cell system, with a grid fraction (real cell system) with successively doubled width and an elementary statistical cell system (imaginary cell system) with a uniform width d_0, is used [49]. After embedding the PSD information in the double statistical cell system, the grading entropy of an arbitrary soil mixture can be computed using [49]:

$$S = -\sum_{i=1}^{N} x_i \log_2 x_i + \sum_{i=1}^{N} x_i \log_2 C_i \tag{4}$$

where N is the number of fractions, x_i is the relative frequency of fraction i, and C_i is the number of elmentary statistical cells in fraction i. The grading entropy S can be expressed as a combination of two terms, the base entropy, S_0, (Eq. 5), and the entropy increment, ΔS, (Eq. 6):

$$S_0 = \sum_{i=1}^{N} x_i \log_2 C_i \tag{5}$$

and

$$\Delta S = -\sum_{i=1}^{N} x_i \log_2 x_i \tag{6}$$

The base entropy, S_0, explains the relative spread of the grain sizes, while the entropy increment, ΔS, describes the statistical entropy of the PSD in terms of the fractions and also explains the relative distribution of the size of the particles.

To make the entropy increment ΔS independent with the number of fractions N, and constrain the base entropy, S_0, and to a set interval for a varying number of fractions [41,44], the normalized grading entropy coordinates, the relative base entropy, A, and the normalised entropy increment, B, were introduced [41]. The relative base entropy, A, describes the symmetry of the PSD and is given by:

$$A = \frac{\sum_{i=1}^{N} x_i (i-1)}{N-1} \tag{7}$$

The normalised entropy increment, B, describes the kurtosis of the PSD, and is given by:

$$B = -\frac{\sum_{i=1}^{N} x_i \log_2 x_i}{\log N} \tag{8}$$

Variations in the PSD can be plotted vectorially as a set of points on the normalized grading entropy diagram rather than a series of full PSD plots.

James [50] undertook an early study on the potential use of the grading entropy co-ordinates as predictors of asphalt concrete k. Feng et al. [18] showed that for a set of constant head permeability tests on road construction granular mixtures (n=30) subjected to similar compaction effort, the normalised grading entropy co-ordinates were a reasonable predictor of k (a similar result was reported in Feng et al. [33] for a database (n=164) of sand-gravel mixtures).

3. Database

A database of asphalt concrete k measurements (n = 1624) has been compiled referred to in this paper as AC/k-1624 (n = 1624). The database is an expanded version of those presented in Vardanega et al. [16] (n = 1318) and Feng [17] (n = 1578). Table 1 shows the origins of the information used to compile the database, relevant ranges of the key parameters and details on the asphalt concrete samples and testing methods. Anisotropy of k is not studied in this paper as the direction of the test flow is not specifically stated in most data sources, and usually the k is measured vertically through the test specimen. Although most of the k data were assessed from laboratory testing on laboratory fabricated samples, the compiled database includes some data from field tests [51,52] as well. However, the field k data will inevitably account for both the horizontal and vertical k to some extent [53,54]. The saturation level of the testing samples is sometimes reported in the data sources [e.g., 53–56]. However, based on an examination of the testing methods used in the database studied it is assumed that the k was measured in saturated or near saturated conditions. The flow conditions during the k test are reported in some sources (see Table 1). Considering the air void level range present in the database (1.7 to 32.67), it is accepted that non-laminar flow may have occurred in some of the tests on samples with higher air voids content. That said, the k-values reported in the database were almost all certainly calculated making use of Darcy's law and the corresponding assumption of laminar flow. Also, some scatter in the analysis results presented in this paper could potentially be due to the variation in test methods and possibly testing temperature, the latter not often reported in the cited publications.

4. Analysis

4.1. Statistical methods

When evaluating the quality of the results of linear regressions, the coefficient of determination (R^2) must be supplemented with other statistical measures, especially the number of data points used in the regression (n) and the standard error (SE) [80]. Phoon and Kulhawy [21,22] explained the importance of quoting the standard deviation of a transformation model (regression) in geotechnical research. For the key correlations presented in this paper, accompanying predicted versus measured plots are provided with the predicted values on the x-axis and the measured values on the y-axis following [81]. Considering the unquantified variations in sample sources, test methods and temperature, a prediction band width of 0.2–5 times range was chosen to examine the prediction accuracy of the datapoints in AC/k-1624. Stevens [82] emphasized the importance of outliers and influential points, as these points may substantially distort the regression results. Datapoints with standardized residuals falling outside the interval (−2.5, 2.5) (e.g., see the review of [83]) and/or with a leverage greater than 3 times of the average (e.g., see the review of [84]) were classed as outliers or influential points. Adjusted correlations were then developed without the identified outliers and influential points included in the analysis. For the three key correlations discussed in Sections 4.2 to 4.4 around 5 to 7% of the points were classed as outliers or influential points using the aforementioned methodology.

4.2. Air voids

The regression between *lnk* and *lnAV%* from AC/k-1624 yielded the following equation:

$$\ln\left[k(mm/s)\right] = 5.37\ln\left[AV(\%)\right] - 15.92$$

$$\left[R^2 = 0.66, SE = 1.75, n = 1624, p < 0.0001\right] \quad (9a)$$

which can be rearranged to give:

$$k(mm/s) = 1.21\times10^{-7}[AV(\%)]^{5.37} \quad (9b)$$

Based on Eq. 9a, about 5% of the datapoints were identified as outliers or influential points. The adjusted correlations with all identified outliers or influential points removed is (Fig. 1):

$$\ln\left[k(mm/s)\right] = 5.54\ln\left[AV(\%)\right] - 16.23$$

$$\left[R^2 = 0.67, SE = 1.56, n = 1542, p < 0.0001\right] \quad (10a)$$

which can be rearranged to:

$$k(mm/s) = 8.94\times10^{-8}[AV(\%)]^{5.54} \quad (10b)$$

Significant differences between the regression coefficients in Eqs. (9a) and (10a) was not observed. The k-measured is plotted against k-predicted using Eq. (10) in Fig. 1 with the k level classified (see the shading on Figs. 1–3 which indicates the following categories based on [15]: A1 = 'very low permeability'; A2 = 'low permeability'; B = 'moderately permeable'; C = 'permeable'; D = 'moderately free draining'; E = 'free draining'). Fig. 1 plot shows that 71.14% of the data points lies within the 0.2 to 5 times range and about 50.06% of the datapoint fall below the line of equality (overpredictions), while 49.94% of the data points are underpredicted by the correlation. Fig. 1 indicates that *AV%* is a strong predictor of k.

4.3. Effective particle size

The coefficient of determination (R^2) for various effective particle sizes (D_{10}, D_{25}, D_{30}, D_{40}, D_{50}, D_{60}, D_{70}, D_{75}, D_{90}) alone used as predictor for k ($\ln k = a\ln D_x + b$) are presented Table 2. It is observed that D_{30} and D_{40} yields the highest R^2, which is close to the results from Waters [85], where D_{25} is chosen as the effective particle size for asphalt concrete k predictions. Table 2 also shows the variation in R^2 when various effective particle sizes (D_{10}, D_{25}, D_{30}, D_{40}, D_{50}, D_{60}, D_{70}, D_{75}, D_{90}) are substituted as D_x in representative pore size (R_p) (see Eq. (2)) then used as predictor. For the studied database (AC/k-1624), D_{60} yields the highest R^2 when adopted as D_x in R_p. Vardanega and Waters [15] showed that the coarse fraction was where the D_{eff} was located (D_{50}-D_{90}) and this is similar to the results shown in Table 2 where R^2 is highest in the range D_{50}-D_{75}. For the analysis in this paper, D_{60} will be used to compute the representative pore size (R_p). The fitted correlation between ln$k$ and lnR_p (D_x= D_{60}) for the entire database yields:

$$\ln\left[k(mm/s)\right] = 3.35\ln\left[R_p(mm)\right] - 0.73$$

$$\left[R^2 = 0.69, SE = 1.65, n = 1624, p < 0.0001\right] \quad (11a)$$

which can be rearranged to give:

$$k(mm/s) = 0.48R_p\ (mm)^{3.35} \quad (11b)$$

where

$$R_p = 2/3\ \times\ \left(AV\%/100\right)\ \times D_{60}(mm)\big) \quad (11c)$$

Around 6.8% of the datapoints were identified as outliers or influential points based on Eq. (11a). The adjusted correlation with these points removed is (Fig. 2):

$$\ln\left[k(mm/s)\right] = 3.34\ln\left[R_p(mm)\right] - 0.57$$

$$\left[R^2 = 0.70, SE = 1.40, n = 1513, p < 0.0001\right] \quad (12a)$$

which can be rearranged to:

$$k(mm/s) = 0.57R_p\ (mm)^{3.34} \quad (12b)$$

Comparing Eqs. (11a) and (12a), it can be observed that the influence from the potential outliers or influential points is marginal. The k-measured versus k-predicted plot using Eq. (12) (Fig. 2) shows that 77.59% of the data points lie within the 0.2 to 5 times prediction range, 43.42% of the data points lie below the line of equality (overprediction),

Table 1
Database sources for AC/k-1624.

Source No.	Reference	n	AV(%) range	AV(%) test method stated in publication	k (mm/s) range	k test method	D_{50} (mm) range	$NMAS$ (mm)***	Notes
S1	Ranieri et al. [57]	12	12.31 to 28.87	-	0.115 to 10.6	UNI- EN 12697/19 (constant head test)	3.54 to 12	7.1 (1), 10 (6), 15 (5)	Data from lab cores
S2	Takahashi and Partl [58]	8	16.3 to 21.8	-	2.18 to 11.47	Falling head test	7.10 to 7.81	14 (2), 16 (2), 11.2 (4)	Data from lab cores
S3	Zhang et al. [59]	56	17.63 to 31.46	Dimensional method, Parafilm method, CoreLok vacuum sealing method and AASHTO T209	0.38 to 8.30	Constant head method VTM-84 and flexible wall falling head method OHD L-44	9.12 to 13.08	19 (26), 25 (30)	Data from lab cores
S4	Jang et al. [60]	10	10.93 to 32.67	-	0.02 to 4.71	-	7.52	12.5 (10)	-
S5**	Kanitpong et al. [61]	62	3.2 to 11	Corelok device	7.10×10^{-7} to 1×10^{-2}	ASTM D5084 (falling head rising-tail test)	1.19 to 2.35	12.5 (36), 19 (26)	Data from lab cores
S6**	Gogula et al. [54]	36	6.2 to 11.6	AASSHTO T209, AASHTO T166	1×10^{-5} to 0.028	Carol-Warner flexible permeameter (falling head test)	1.80 to 6.48	12.5 (18), 19 (18)	Data from lab cores. Authors state that flow of the permeant was assumed to be laminar.
S7	Setyawan [62]	12	23.78 to 27.74	-	0.94 to 1.61	-	6.05 to 7.16	9.5 (2), 11.2 (10)	Data from lab cores
S8	Sprinkel and Apeagyei [63]	42	2.9 to 7.47	ASSHTO T166	1×10^{-6} to 3.58×10^{-2}	VTM 120 (falling head test)	2.55 to 3.13	9.5 (42)	Data from both lab and field cores
S9	Putman [64]	10	10 to 22.1	ASTM D7063	0.30 to 4.80	Modified ASTM PS129 (falling head test)	4.9 to 10.33	9 (1), 9.5 (2), 11.2 (1), 12.5 (5), 19 (1)	Data from lab cores
S10	Kutay et al. [23]	43	1.7 to 23.1	-	6×10^{-4} to 12.67	Bubble tube constant head permeameter	1.48 to 12.5	9.5 (10), 12.5 (17), 19 (10), 25 (6)	Data from both lab and field cores. Authors used a numerical model to show that the flow of the permeant under experimental conditions was likely to be laminar.
S11**	Aboufoul and Garcia [11]	38	8.7 to 26	BS EN 12679	1.6×10^{-3} to 5.11	Florida falling head method	8.2 to 11.76	14 (3), 16 (32), 20 (3)	Data from lab cores. Authors present a literature review highlighting the assumption of laminar flow in testing for asphalt concrete k
S12	Feng [17]	3	9.2 to 9.6	WA732.2-2011, WA733.1-2012	4.76×10^{-3} to 3.60×10^{-1}	Ponding method (falling head test)	5.30 to 6.19	10(1), 11.5 (2)	Data from lab cores
S13**	Choubane et al. [55,65]	151	1.9 to 14.6	FM 1-T 166 and FM 1-T 209	1×10^{-4} to 0.10	Florida falling head method	1.85 to 10.42	19 (64), 16 (1), 12.5 (83), 9.5 (3)	Data from both lab and field cores, 8 zero permeability values were removed from the original source
S14	Al-Omari et al. [6]	13	9.03 to 18.04	AASHTO T-166 and Corelok device	0.02 to 3.24	Karol-Warner permeameter (falling head test)	4.27 to 6.73	12.5 (8), 19 (2), 25 (3)	Data from lab cores, the adopted AV% are the averaged values of both test methods, 2 zero permeability values were removed from the original source
S15	Bhattacharjee and Mallick [66]	90	4.58 to 12.4	AASHTO T 209-99, AASHTO T 166-88 (saturated surface dry method) and Vacuum seal method	3.7×10^{-4} to 0.315	Florida falling head method	2.74 to 7.82	9.5 (27), 12.5 (45), 19 (18)	Data from lab cores, the adopted AV% are the averaged values of both test methods

(*continued on next page*)

Table 1 (*continued*)

Source No.	Reference	n	AV(%) range	AV(%) test method stated in publication	k (mm/s) range	k test method	D_{50} (mm) range	$NMAS$ (mm)***	Notes
S16**	Brown et al. [67-70]	367	3.85 to 20.47	AASHTO T166 and vacuum seal device	1×10^{-4} to 1.28	ASTM PS 129-01 (falling head test)	1.33 to 10.72	9.5 (120), 12.5 (186), 19 (61)	Data from both lab and field cores, 41 zero permeability values were removed from the original source
S17	Haddock et al. [71]	5	10.4 to 13.8	AASHTO T166 and AASHTO T209	1.9×10^{-3} to 7.84×10^{-2}	Florida falling head method	3.65	9 (5)	Data from filed cores, adopted PSD is the averaged value of EB and WB lanes
S18**	Chen et al. [56]	40	1.80 to 20.22	AASHTO T 269	4.47×10^{-5} to 7.84×10^{-2}	Falling head test	5.74 to 13.29	19 (40)	Data from lab cores
S19**	Norambuena-Contreras et al. [72]	72	4.26 to 20.51	Geometric	1.9×10^{-6} to 3.83	BS 1377-6 (constant head test); ASTM D5084 method B (falling head test)	4.57 to 7.29	11.2 (18), 16 (54)	Data from lab cores, k test method reported as ASTM D5086 in the original source, believed to be a typo here. The authors state the laminar flow assumption
S20**	Pease et al. [73]	6	4 to 6.8	-	3.63×10^{-5} to 9.45×10^{-4}	ASTM D5084 method C (falling head rising-tail test)	2.17 to 2.22	11.2 (2), 12.5 (4)	Data from field cores
S21**	Yan et al. [74]	51	4.3 to 11.9	-	1×10^{-5} to 2.45	Florida falling head method (FM 5-565)	1.11 to 2.32	9.5 (12), 12.5 (6), 19 (14), 25 (6), 37.5 (13)	Data from lab cores. The author state that k was calculated using the laminar flow assumption.
S22*	Schmitt et al. [52]	19	3.4 to 4.1	-	1×10^{-5} to 3.9×10^{-4}	NCAT device	1.37 to 3.53	9 (2), 10 (1), 11.2 (10), 12.5 (6)	Data from filed core, 1 zero permeability values were removed from the original source
S23	Hewitt [75]	27	5.22 to 16.42	-	2×10^{-4} to 0.49	Ponding method (falling head test)	3.91 to 5.46	9 (9), 9.5 (9), 11.2 (9)	Data from lab cores
S24	Maupin [76,77]	218	4.8 to 16.98	ASTM D3203	2.69×10^{-4} to 0.64	Falling head permeability test	2.72 to 5.32	9.5 (68), 12.5 (150)	Data from both lab and field cores
S25*	Cooley et al. [51]	131	2.38 to 13.61	-	1.45×10^{-4} to 0.61	Field permeameter	3.44 to 12.2	9.5 (29), 12.5 (47), 19 (20), 25 (35)	Data from field cores
S26**	Mallick et al. [53]	49	2.2 to 12.3	-	6.35×10^{-5} to 1.23	Florida falling head method (FM 5-565)	2.16 to 6.23	9.5 (20), 12.5 (10), 19 (9), 25 (10)	Data from field cores, the adopted permeability value is the lab permeability, 6 zero permeability values were removed from the original source
S27	Vardanega et al. [78]	53	4.8 to 10	-	3.00×10^{-3} to 0.26	Main Roads Material Test Method Q304-2002 (falling head test)	3.5 to 6.35	14 (53)	Data from lab cores. Mix A not included see [15] and 2 Mix B centreline (CL) points with near zero outlier k values not included in the database
Summary									
Maximum value			32.67		12.67		13.29	37.5	
Minimum value			1.7		7.10×10^{-7}		1.19	7.1	
Mean value			9.49		0.30		5.08	14.17	
Standard deviation			4.85		1.06		2.59	4.68	
Coefficient of Variation			0.51		3.56		0.51	0.33	

Sources with explicitly stated saturation level.

Notes: Data sources S23-S27 and part of the data in S5 (also in [79]) were used in Vardanega and Waters [15]; S13-S22 in Vardanega et al [16] and S4-S12 in Feng [17] and Feng et al. [33].

* Field permeability test data.

** Sources with saturation level clearly stated.

*** Number in brackets is the n value for the NMAS value stated.

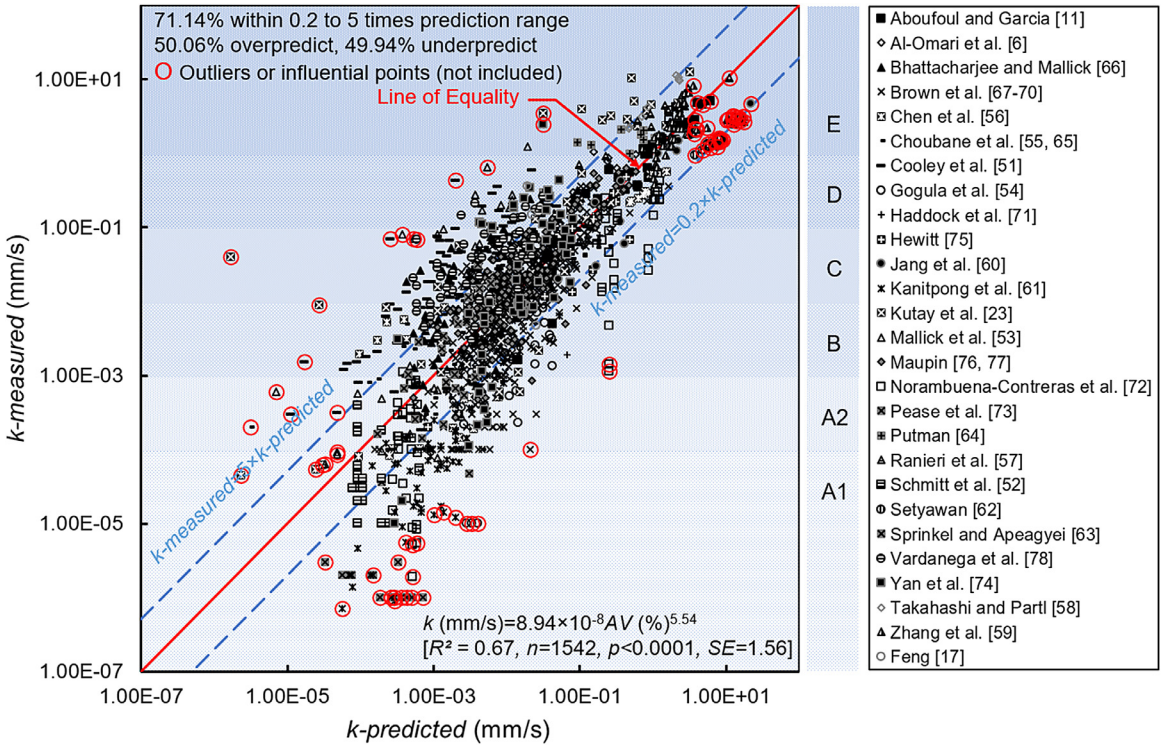

Fig. 1. *k*-measured versus *k*-predicted using Eq. (10b) (statistical measures relate to Eq. (10a) i.e. linear form with logarithmic transforms) (Shading indicates the following categories: A1 = 'very low permeability'; A2 = 'low permeability'; B = 'moderately permeable'; C = 'permeable'; D = 'moderately free draining'; E = 'free draining' - categorisation based on Vardanega and Waters [15]).

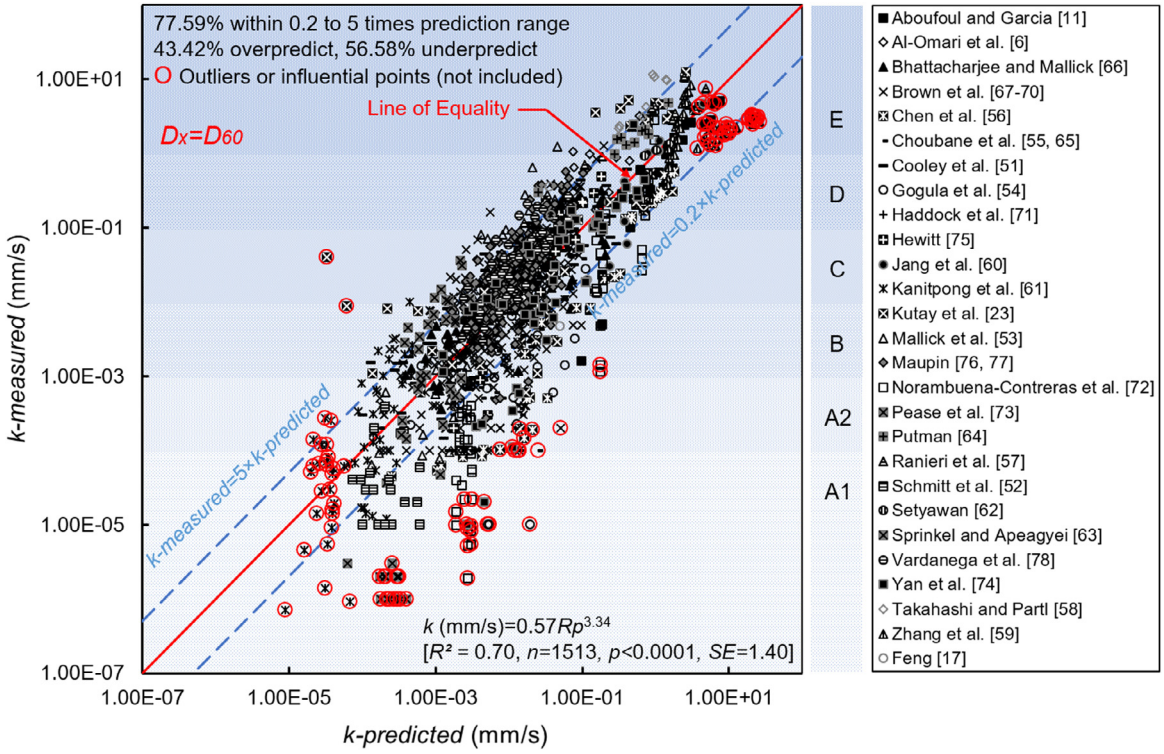

Fig. 2. *k*-measured versus *k*-predicted using Eq. (12b) (statistical measures relate to Eq. (12a) i.e. linear form with logarithmic transforms) (R_p is expressed in mm) (Shading indicates the following categories: A1 = 'very low permeability'; A2 = 'low permeability'; B = 'moderately permeable'; C = 'permeable'; D = 'moderately free draining'; E = 'free draining' - categorisation based on Vardanega and Waters [15]).

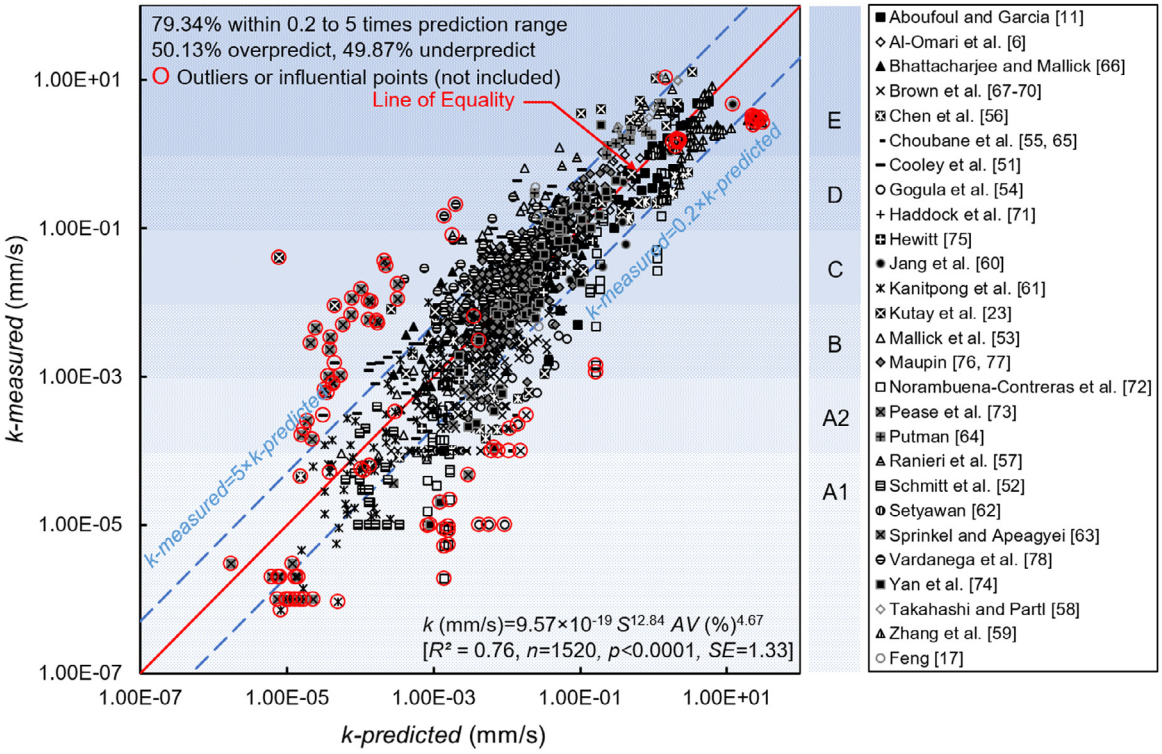

Fig. 3. *k*-measured versus *k*-predicted using Eq. (14b) (statistical measures relate to Eq. (14a) i.e. linear form with logarithmic transforms) (Shading indicates the following categories: A1 = 'very low permeability'; A2 = 'low permeability'; B = 'moderately permeable'; C = 'permeable'; D = 'moderately free draining'; E = 'free draining' - categorisation based on Vardanega and Waters [15]).

Table 2
R^2 for various effective particle size *Dx* based on the entire database (*k* expressed in mm/s).

	R^2									
D_x(mm)	10	20	25	30	40	50	60	70	75	90
$lnk = a lnD_x + b$	0.20	0.32	0.33	0.35	0.35	0.34	0.31	0.27	0.25	0.17
$lnk = a lnR_p + b$	0.42	0.56	0.59	0.63	0.67	0.69	0.69	0.69	0.69	0.65

while the remainder (56.58%) of the data points lie above the line of equality (underprediction). Fig. 2 shows that the inclusion of gradation parameter (D_x) does slightly enhance the accuracy of prediction in terms of R^2 and percentage within prediction range when compared with data using *AV%* alone (especially for the permeable and free draining categories), though not as marked as presented in the earlier study [15].

4.4. Grading entropy

The grading entropy *S* explains the disorder of the PSDs [44,45,49]. Based on its intrinsic features, it is reasonable to infer that the grading entropy (*S*) could assist with characterization of the fluid path within asphalt concrete mixtures. The target PSD and *AV%* of asphalt concrete mixtures are usually specified in the field so these parameters were considered good candidates to predict *k*. The multiple linear regression of *k* with both *AV%* and *S* yields:

$$\ln\left[k(mm/s)\right] = 4.70\ln\left[AV(\%)\right] + 10.52\ln S - 36.69$$

$$\left[R^2 = 0.72, SE = 1.56, n = 1624, p < 0.0001\right] \quad (13a)$$

which can be rearranged to give:

$$k(mm/s) = 1.16 \times 10^{-16}[AV(\%)]^{4.70} S^{10.52} \quad (13b)$$

Based on Eq. 13a, 6.4% of the points in the studied database can be identified as outliers or influential points. The adjusted regression with these points removed is (Fig. 3):

$$\ln\left[k(mm/s)\right] = 4.67\ln\left[AV(\%)\right] + 12.84\ln S - 41.49$$

$$\left[R^2 = 0.76, SE = 1.33, n = 1520, p < 0.0001\right] \quad (14a)$$

which can be rearranged to:

$$k(mm/s) = 9.57 \times 10^{-19}[AV(\%)]^{4.67} S^{12.84} \quad (14b)$$

Some variations on the regression coefficients can be observed especially on *S*. The *k*-measured versus *k*-predicted (Eq. (14)) plot is presented in Fig. 3, where 79.34% of the data points lie within the 0.2 to 5 times prediction range and 50.13% of the points fall below the line of equality (overpredictions), and 49.87% of the data points lie above (underpredictions). Fig. 3 shows that Eq. (14) gives a better prediction of *k* compared to Eq. (12) and Eq. (10).

5. Analysis of data subsets

In the following analysis, the entire database AC/k-1624 is used to study whether the test method, gradation classification and *NMAS* significantly impact the regression results presented in Section 4. The outliers identified in Section 4 are not removed in the analysis that follows, as the outliers and influential points will be slightly different for each data subset. Therefore, the regression results from the sub dataset analysis should be compared with the fitted results based on the entire database (Eqs. (9b), (11b), (13b)).

Table 3
Analysis result of data subsets classified by test type (all results $p < 0.0001$) (SE values correspond to the ln-ln form of the regression).

Test method	Calibrated equation (k expressed in mm/s and R_p in mm)	n	R^2	SE	% within 0.2x to 5x region	% Overpredicted	% Underpredicted
constant head test	$k = 2.29 \times 10^{-8} AV(\%)^{6.16}$	117	0.80	2.08	73.50%	53.85%	46.15%
	$k = 0.50 R_p^{4.18} (D_x = D_{60})$	117	0.76	2.30	64.96%	48.72%	51.28%
	$k = 9.51 R_p^{2.56} (D_x = D_{20})$	117	0.80	2.07	64.10%	55.56%	44.44%
	$k = 1.68 \times 10^{-7} AV(\%)^{6.19} S^{-0.96}$	117	0.80	2.09	74.36%	53.85%	46.15%
falling head test	$k = 1.90 \times 10^{-7} AV(\%)^{5.17}$	1267	0.63	1.59	74.11%	46.72%	53.28%
	$k = 0.42 R_p^{3.23} (D_x = D_{60})$	1267	0.62	1.60	74.98%	41.28%	58.72%
	$k = 0.25 R_p^{3.48} (D_x = D_{70})$	1267	0.62	1.59	74.90%	40.49%	59.51%
	$k = 9.00 \times 10^{-15} AV(\%)^{4.59} S^{8.58}$	1267	0.67	1.49	77.27%	44.91%	55.09%
falling head rising tail test	$k = 5.12 \times 10^{-10} AV(\%)^{7.07}$	68	0.71	1.15	83.82%	51.47%	48.53%
	$k = 1.03 R_p^{3.57} (D_x = D_{60})$	68	0.45	1.58	67.75%	44.12%	55.88%
	$k = 7.41 R_p^{3.97} (D_x = D_{50})$	68	0.48	1.54	73.53%	44.12%	55.88%
	$k = 1.12 \times 10^{-11} AV(\%)^{7.02} S^{2.03}$	68	0.71	1.15	83.82%	48.53%	51.47%
field permeability test	$k = 7.46 \times 10^{-7} AV(\%)^{5.02}$	150	0.57	1.74	60.67%	50.67%	49.33%
	$k = 1.56 R_p^{3.94} (D_x = D_{60})$	150	0.81	1.17	84.67%	46.00%	54.00%
	$k = 2.83 R_p^{3.57} (D_x = D_{50})$	150	0.84	1.07	89.33%	43.33%	56.67%
	$k = 2.40 \times 10^{-30} AV(\%)^{4.36} S^{25.90}$	150	0.84	1.07	87.33%	48.00%	52.00%

Table 4
Analysis result of data subsets classified by gradation type (two categories) (all results $p < 0.0001$) (SE values correspond to the ln-ln form of the regression).

Gradation type	Calibrated equation (k expressed in mm/s and R_p in mm)	n	R^2	SE	% within 0.2x to 5x region	% Overpredicted	% Underpredicted
Well graded	$k = 2.93 \times 10^{-7} AV(\%)^{5.02}$	891	0.55	1.62	71.27%	50.84%	49.16%
	$k = 0.94 R_p^{3.84} (D_x = D_{60})$	891	0.58	1.57	75.76%	39.96%	60.04%
	$k = 8.48 \times 10^{-19} AV(\%)^{4.97} S^{12.56}$	891	0.60	1.52	75.53%	46.35%	53.65%
Poorly graded	$k = 5.83 \times 10^{-8} AV(\%)^{5.62}$	733	0.72	1.87	67.39%	46.25%	53.75%
	$k = 0.38 R_p^{3.22} (D_x = D_{60})$	733	0.77	1.71	72.17%	41.06%	58.94%
	$k = 1.67 \times 10^{-16} AV(\%)^{4.55} S^{10.52}$	733	0.80	1.60	73.81%	44.61%	55.39%

Table 5
Analysis result of data subsets classified by gradation type (four categories) (all results $p < 0.0001$) (SE values correspond to the ln-ln form of the regression).

Gradation type	Calibrated equation (k expressed in mm/s and R_p in mm)	n	R^2	SE	% within 0.2x to 5x region	% Overpredicted	% Underpredicted
Well graded gravel	$k = 4.41 \times 10^{-6} AV(\%)^{4.19}$	322	0.50	1.64	72.67%	44.41%	55.59%
	$k = 0.71 R_p^{3.76} (D_x = D_{60})$	322	0.53	1.60	75.47%	42.55%	57.45%
	$k = 1.55 R_p^{3.60} (D_x = D_{50})$	322	0.54	1.58	75.16%	41.93%	58.07%
	$k = 2.33 \times 10^{-13} AV(\%)^{4.12} S^{7.81}$	322	0.52	1.62	74.53%	44.10%	55.90%
Poorly graded gravel	$k = 4.91 \times 10^{-6} AV(\%)^{4.08}$	364	0.73	1.35	82.14%	45.60%	54.40%
	$k = 0.33 R_p^{3.18} (D_x = D_{60})$	364	0.71	1.38	81.04%	42.03%	57.97%
	$k = 0.22 R_p^{3.27} (D_x = D_{70})$	364	0.72	1.36	81.32%	40.93%	59.07%
	$k = 7.86 \times 10^{-14} AV(\%)^{3.85} S^{8.56}$	364	0.76	1.28	83.79%	46.15%	53.85%
Well graded sand	$k = 8.33 \times 10^{-8} AV(\%)^{5.38}$	569	0.64	1.32	80.84%	43.94%	56.06%
	$k = 2.39 R_p^{4.44} (D_x = D_{60})$	569	0.52	1.52	77.50%	41.48%	58.52%
	$k = 3.33 \times 10^{-7} AV(\%)^{5.37} S^{-0.65}$	569	0.64	1.33	81.20%	44.29%	55.71%
Poorly graded sand	$k = 7.15 \times 10^{-9} AV(\%)^{6.40}$	369	0.60	1.91	65.85%	44.99%	55.01%
	$k = 0.83 R_p^{3.63} (D_x = D_{60})$	369	0.58	1.96	65.04%	39.84%	60.16%
	$k = 2.45 R_p^{3.61} (D_x = D_{50})$	369	0.60	1.91	67.48%	38.75%	61.25%
	$k = 5.63 \times 10^{-15} AV(\%)^{5.61} S^{7.68}$	369	0.66	1.77	70.46%	46.88%	53.12%

5.1. Test method

The database AC/k-1624 includes k data measured by various test methods. In order to investigate the effect of the test method, the database is further divided into 'constant head', 'falling head', 'falling head rising-tail', 'field test' subsets. For the 'constant head test' subset, D_{20} gives the highest R^2, while for the other subsets, the peaks are between D_{50} and D_{70}. The analysis results using Eqs. (9b), (11b), (13b) and modified Eq. (11b) with the favoured D_x for each data subsets are summarized in Table 3. The examined models (Eqs. (9b), (11b) and (13b)) still provide statistically strong predictions mostly between 0.2 to 5 times range, though some degree of variation appears in the coefficient and the exponent of the regressed Eqs. among different subsets. Most of the data is from falling-head tests ($n = 1267$) and it is therefore not surprising that the regression coefficients are similar to those shown in Eqs. (9b), (11b) and (13b).

5.2. Gradation parameter

O'Kelly and Nogal [20] processed data from 47 permeability measurements on granular soil and concluded that for the hydraulic conductivity assessment of coarse-grained soils separate analysis should be conducted based on the gradation type. The asphalt concrete mixture is largely comprised of coarse-grained soil, it is thus worth examining the potential influence brought by the gradation types for the asphalt concrete database in this study. As per the Unified Soil Classification System [88], the database AC/k-1624 was initially divided into well-graded soil and poorly-graded soil based on the gradation type (Table 4), and then further subdivided into well-graded gravel, poorly-graded gravel, well-graded sand and poorly-graded sand data subsets based on the fraction size (Table 5). The most favoured D_x always falls within D_{50} to D_{70} range for all subsets. The analysis results calibrated based on Eqs. (9b), (11b), (13b) and modified Eq. (11b) with the favoured

Table 6
Analysis result of data subsets classified by *NMAS* (all results $p < 0.0001$) (SE values correspond to the ln-ln form of the regression).

NMAS	Calibrated equation (k expressed in mm/s and R_p in mm)	n	R^2	SE	% within 0.2x to 5x region	% Overpredicted	% Underpredicted
NMAS≤ 9.5mm	$k = 7.82 \times 10^{-9} AV(\%)^{6.46}$	362	0.75	1.41	78.73%	45.03%	54.97%
	$k = 3.43 R_p^{4.42} (D_x = D_{60})$	362	0.71	1.52	79.28%	43.65%	56.35%
	$k = 0.56 R_p^{5.94} (D_x = D_{90})$	362	0.77	1.36	82.60%	46.69%	53.31%
	$k = 3.07 \times 10^{-13} AV(\%)^{5.76} S^{5.69}$	362	0.77	1.36	80.66%	48.07%	51.93%
9.5mm< NMAS≤ 12.5mm	$k = 1.15 \times 10^{-7} AV(\%)^{5.35}$	695	0.67	1.52	75.40%	47.05%	52.95%
	$k = 0.70 R_p^{3.51} (D_x = D_{60})$	695	0.72	1.39	79.14%	43.02%	56.98%
	$k = 1.52 \times 10^{-20} AV(\%)^{4.80} S^{14.64}$	695	0.74	1.33	79.86%	47.05%	52.95%
NMAS>12.5m	$k = 4.52 \times 10^{-7} AV(\%)^{4.96}$	567	0.63	2.05	56.97%	46.03%	53.97%
	$k = 0.29 R_p^{3.38} (D_x = D_{60})$	567	0.71	1.81	67.20%	44.62%	55.38%
	$k = 0.54 R_p^{3.15} (D_x = D_{50})$	567	0.72	1.79	67.02%	45.33%	54.67%
	$k = 5.03 \times 10^{-20} AV(\%)^{4.19} S^{14.57}$	567	0.70	1.84	67.02%	46.74%	53.26%

D_x for each data subsets are summarized in Tables 4 and 5. Relatively minor variations can be observed on the exponents and coefficients for the calibrated models (with the exception of 'well-graded sand'). The transformation model calibrated using Eq. (13b) yields either the highest R^2 and/or the largest percentage of the prediction within 0.2 to 5 times range for most subsets. The calibrated Eqs. (9b), (11b) and (13b) all provide statistically strong predictions of k generally within 0.2 to 5 times the prediction ranges for the sub-datasets presented in Tables 4 and 5.

5.3. Nominal maximum aggregate size (NMAS)

The effect of nominal maximum aggregate size (*NMAS*) on the k of asphalt concrete has been discussed in Hainin et al. [5] and Yan et al. [74]. AC/k-1624 was subdivided into three data subsets based on the *NMAS* and its potential effect on the prediction of k is further investigated. Table 6 shows that for data subsets with coarser *NMAS* (*9*.5mm< *NMAS*≤ 12.5mm and *NMAS* > 12.5mm) the most favoured D_x still falls within D_{50} to D_{70} range, while for data subset with *NMAS*≤ 9.5mm, D_{90} gives the peak value in R^2. The analysis results calibrated based on Eqs. (9b), (11b), (13b) and modified Eq. (11b) with the favoured D_x for each data subset are summarized in Tables 6. Some degree of variation in the regression coefficients does exist among different data subsets but not as marked as for test type (Table 3).

6. Summary and conclusions

A large database ($n = 1624$) of k measurements on asphalt concrete called AC/k-1624 has been presented in this paper. Potential predictors for k of asphalt concrete include *AV%*, effective particle size D_x, representative pore size R_p, grading entropy parameter (S), gradation parameters and *NMAS* were investigated using AC/k-1624. *AV%* is a significant predictor of asphalt concrete permeability explaining around 67% of the variation (R^2=0.67, Eq. (10)). An effective particle size is often used to incorporate gradation into empirical models for asphalt concrete permeability e.g. the representative pore size [15] or normalised air voids concepts [2]. Such methods are limited by the need to statistically determine the best D_{eff} which may change as the database expands (D_{75} was chosen in [15] with further research in this paper showing D_{60} may be a better candidate). The grading entropy framework in the form of the S parameter offers for a large database n >1500 (with outliers removed) a method to incorporate gradation without having to statistically determine the effective particle size. Inclusion of S explains a further 9 percent variation in k (R^2=0.76, Eq. (14)) as opposed to only 3 percent for R_p (R^2=0.70, Eq. (12)).

Eq. (14) is a novel empirical equation which systematically captures the grading and porosity information of asphalt concrete mixtures, calibrated with a large database AC/k-1624 (see also Ching et al. [86] for recent developments in international efforts to develop geodatabases for key geotechnical parameters or regions). The present authors suggest that a similar approach can be used for pavement engineering properties either at international or regional scale. Eq. (14) shows that from both statistically and practically perspectives S is a superior way of accounting for gradation changes than the R_p concept for asphalt concrete (based on the analysis of a large database AC/k-1624). Subdivision of the database by test type, grading classification and *NMAS* shows that no significant increases in R^2 can be found from Eq. (14) with the exception of constant head and field tests (Table 3), although it is noted that the regression equations are affected to some degree by these subdivisions.

While the statistical trends shown in this paper are significant (p is often < 0.001) and the database is relatively large (n > 1600) much of the scatter is probably due to the fact that different test methods for k and *AV(%)* determination were used in the studies included in the database. While it would be preferable to have a database with limited variation of conditions, such dataset is not available at present. Despite this limitation, the trends shown give useful approximations for k that can be used by pavement engineers to assess the propensity for different mix design to transmit water. Future uses of large databases such as AC/k-1624 may include Artificial Neural Network (ANN) modelling approaches as reported in [38,87].

Disclosure statement

The authors wish to report no conflict of interest.

Data availability statement

This research has not generated any new experimental data.

Declaration of Competing Interest

The authors declare that they have no known competing financial interests or personal relationships that could have appeared to influence the work reported in this paper.

Acknowledgements

The first author was supported by a scholarship from the China Scholarship Council (CSC) [grant number 201708060067].

References

[1] A. Dawson, N. Kringos, T. Scarpas, P. PavšičA Dawson (Ed.), Water in the Pavement Surfacing, Water in Road Structures 5 (2009) 81–105, doi:10.1007/978-1-4020-8562-8_5.
[2] T.J. Waters, A study of water infiltration through asphalt road surface materials, in: International symposium on subdrainage in roadway pavements and subgrades, 1998, pp. 311–317.
[3] B. Huang, L.N. Mohammad, A. Raghavendra, C. Abadie, Fundamentals of permeability in asphalt mixtures, J. Assoc. Asph. Paving Technol. 68 (1999) 479–500.
[4] M. R. Hainin, L. A. Cooley Jr., B. D. Prowell, An investigation of factors influencing permeability of Superpave mixes, Paper presented at: 82nd Annu. Meet. Transp. Res. Board, Washington, DC, (2003).

[5] M.R. Hainin, N.I.M. Yusoff, M.K.I. Mohd Satar, E.R. Brown, The effect of lift thickness on permeability and the time available for compaction of hot mix asphalt pavement under tropical climate condition, Constr. Build. Mater. 48 (2013) 315–324, doi:10.1016/j.conbuildmat.2013.06.092.

[6] A. Al-Omari, L. Tashman, E. Masad, A. Cooley, T. Harman, Proposed methodology for predicting HMA permeability, J. Assoc. Asph. Paving Technol. 71 (2002) 30–58.

[7] A. Al-Omari, E. Masad, Three dimensional simulation of fluid flow in X-ray CT images of porous media, Int. J. Numer. Anal. Methods Geomech. 28 (13) (2004) 1327–1360, doi:10.1002/nag.389.

[8] A. Nataatmadja, The use of hyperbolic function for prediction critical permeability of asphalt, in: Proceedings 24th ARRB Conference – Building on 50 Years of Road and Transport Research, Melbourne, VIC, Australia, 2010.

[9] A. Bhargava, A. Das, R. Srivastava, Estimation of permeability of porous asphalt mix, Proc. Inst. Civ. Eng. - Transp. 165 (4) (2012) 303–310, doi:10.1680/tran.10.00070.

[10] P.J. Vardanega, State of the art: permeability of asphalt concrete, J. Mater. Civ. Eng. 26 (1) (2014) 54–64, doi:10.1061/(ASCE)MT.1943-5533.0000748.

[11] M. Aboufoul, A. Garcia, Factors affecting hydraulic conductivity of asphalt mixture, Mater. Struct. 50 (2) (2017) 116, doi:10.1617/s11527-016-0982-6.

[12] M. Fang, D. Park, J.L. Singuranayo, H. Chen, Y. Li, Aggregate gradation theory, design and its impact on asphalt pavement performance: a review, Int. J. Pavement Eng. 20 (12) (2019) 1408–1424, doi:10.1080/10298436.2018.1430365.

[13] S.A. Blaauw, J.W. Maina, E. Horak, Towards a mix design model for the prediction of permeability of hot-mix asphalt, Constr. Build. Mater. 221 (2019) 637–642, doi:10.1016/j.conbuildmat.2019.06.082.

[14] S. Chen, S. Adhikari, Z. You, Relationship of coefficient of permeability, porosity, and air voids in fine-graded HMA, J. Mater. Civ. Eng. 31 (1) (2019) 04018359, doi:10.1061/(asce)mt.1943-5533.0002573.

[15] P.J. Vardanega, T.J. Waters, Analysis of asphalt concrete permeability data using representative pore size, J. Mater. Civ. Eng. 23 (2) (2011) 169–176, doi:10.1061/(ASCE)MT.1943-5533.0000151. and Erratum, 27(8) (2015), [08215002], doi: 10.1061/(ASCE)MT.1943-5533.0001369.

[16] P.J. Vardanega, S. Feng, C.J. Shepheard, et al., Some recent research on the hydraulic conductivity of road materials, in: bearing capacity of roads, railways and airfields, in: A Loizos, et al. (Eds.), Proceedings of the 10th International Conference on the Bearing Capacity of Roads, Railways and Airfields (BCRRA 2017), Athens, Greece, June 28-30, 2017, London, UK, Taylor & Francis, 2017, pp. 135–142.

[17] S. Feng, Assessing the Permeability of Pavement Construction Materials by Using Grading Entropy Theory, MSc Thesis, University of Bristol, Bristol, UK, 2017.

[18] S. Feng, P.J. Vardanega, E. Ibraim, I. Widyatmoko, C. Ojum, Permeability assessment of some granular mixtures, Géotechnique 69 (7) (2019) 646–654, doi:10.1680/jgeot.17.T.039.

[19] S. Feng, P.J. Vardanega, E. Ibraim, I. Widyatmoko, C. Ojum, B.C. O'Kelly, M. Nogal, Discussion: permeability assessment of some granular mixtures, Géotechnique 70 (9) (2020) 845–847, doi:10.1680/jgeot.19.D.005.

[20] B.C. O'Kelly, M. Nogal, Determination of soil permeability coefficient following an updated grading entropy approach, Geotech. Res. 7 (1) (2020) 58–70, doi:10.1680/jgere.19.00036.

[21] K.K. Phoon, F.H. Kulhawy, Characterization of geotechnical variability, Can. Geotech. J. 36 (4) (1999) 612–624, doi:10.1139/t99-038.

[22] K.K. Phoon, F.H. Kulhawy, Evaluation of geotechnical property variability, Can. Geotech. J. 36 (4) (1999) 625–639, doi:10.1139/t99-039.

[23] M.E. Kutay, A.H. Aydilek, E. Masad, T. Harman, Computational and experimental evaluation of hydraulic conductivity anisotropy in hot-mix asphalt, Int. J. Pavement Eng. 8 (1) (2007) 29–43, doi:10.1080/10298430600819147.

[24] M.E. Kutay, A.H. Aydilek, E. Masad, Estimating directional permeability of HMA based on numerical simulation of micro-scale water flow, J. Transp. Res. Board (2007) 29–36, doi:10.3141/2001-04.

[25] J. Chen, X. Yin, H. Wang, X. Ma, Y. Ding, G. Liao, Directional distribution of three-dimensional connected voids in porous asphalt mixture and flow simulation of permeability anisotropy, Int. J. Pavement Eng. (2018), doi:10.1080/10298436.2018.1555330.

[26] G. Ferreira, W.L.C. Branco, V.T.F S. Caro, K. Vasconcelos, Analysis of Water Flow in an Asphalt Pavement Surface Layer with Different Thicknesses and Different Permeability Coefficients, Road Mater, 2019, doi:10.1080/14680629.2019.1617186.

[27] D.W. Taylor, Fundamentals of Soil Mechanics, John Wiley& Son Inc, New York, 1948.

[28] E. Zube, Compaction of asphalt concrete pavement as related to the water permeability test, in: Proceedings 41st Annual Meeting Highway Research Board, 1962, pp. 12–37.

[29] J. Kozeny, Über kapillare Leitung des Wassers im Boden:(Aufstieg, Versickerung und Anwendung auf die Bewässerung), Hölder-Pichler-Tempsky, 1927 (in German).

[30] P.C. Carman, The determination of the specific surface of powders, J. Soc. Chem. Ind. 57 (1938) 225–234.

[31] P.C. Carman, Flow of Gases Through Porous Media, Butterworths Scientific Publications, London, 1956.

[32] R.A. Tarefder, M. Ahmad, Evaluation of pore structure and its influence on permeability and moisture damage in asphalt concrete, Int. J. Pavement Eng. 18 (3) (2017) 274–283, doi:10.1080/10298436.2015.1065995.

[33] S. Feng, P.J. Vardanega, E. Ibraim, I. Widyatmoko, C. Ojum, Assessing the hydraulic conductivity of road paving materials using representative pore size and grading entropy, ce/papers 2 (2–3) (2018) 871–876, doi:10.1002/cepa.780.

[34] H. Xu, Y. Tan, X. Yao, X-ray computed tomography in hydraulics of asphalt mixtures: procedure, accuracy, and application, Constr. Build. Mater. 108 (2016) 10–21, doi:10.1016/j.conbuildmat.2016.01.032 .

[35] H. Xu, X. Yao, D. Wang, Y. Tan, Investigation of anisotropic flow in asphalt mixtures using the X-ray image technique: pore structure effect, Road Mater. Pavement Des. 20 (3) (2019) 491–508, doi:10.1080/14680629.2017.1397047.

[36] J. Hu, Z. Qian, P. Liu, D. Wang, M. Oeser, Investigation on the permeability of porous asphalt concrete based on microstructure analysis, Int. J. Pavement Eng. (2019), doi:10.1080/10298436.2018.1563785.

[37] F.J. Sánchez-Leal, Gradation chart for asphalt mixes: development, J. Mater. Civ. Eng. 19 (2) (2007) 185–197, doi:10.1061/(asce)0899-1561(2007)19:2(185).

[38] R.A. Tarefder, L. White, M. Zaman, Neural network model for asphalt concrete permeability, J. Mater. Civ. Eng. 17 (1) (2005) 19–27, doi:10.1061/(asce)0899-1561(2005)17:1(19).

[39] A. Gaxiola, A. Ossa, Hydraulic, volumetric, and mechanical approach in asphalt mixture design for impervious barriers, J. Mater. Civ. Eng. 31 (2) (2019) 04018396, doi:10.1061/(ASCE)MT.1943-5533.0002613.

[40] T. J. Waters, A Study of Water Infiltration through asphalt road surface materials, paper presented at road system and engineering technology forum 2004: Right outcome, right technology, Bardon, Brisbane, Queensland, Australia, 4–6 August 2004.

[41] V.P. Singh, Entropy Theory in Hydraulic Engineering, American Society of Civil Engineers, Reston, VA, USA, 2014, pp. 299–358.

[42] C.E. Shannon, A mathematical theory of communication, Bell Syst. Tech. J. 27 (3) (1948) 379–423, doi:10.1002/j.1538-7305.1948.tb01338.x.

[43] J.R. McDougall, E. Imre, D. Barreto, D. Kelly, Volumetric consequences of particle loss by grading entropy, Géotechnique 63 (3) (2013) 262–266, doi:10.1680/geot.sip13.t.002.

[44] J. Lőrincz, E. Imre, M. Gálos, Q.P. Trang, K. Rajkai, S. Fityus, G. Telekes, Grading entropy variation due to soil crushing, Int. J. Geomech. 5 (4) (2005) 311–319, doi:10.1061/(asce)1532-3641(2005)5:4(311).

[45] E. Imre, J. Lőrincz, J. Szendefy, P.Q. Trang, L. Nagy, V.P. Singh, S. Fityus, Case studies and benchmark examples for the use of grading entropy in geotechnics, Entropy 14 (6) (2012) 1079–1102, doi:10.3390/e14061079.

[46] E. Imre, L. Nagy, J. Lőrincz, N. Rahemi, T. Schanz, V. Singh, S. Fityus, Some comments on the entropy-based criteria for piping, Entropy 17 (4) (2015) 2281–2303, doi:10.3390/e17042281.

[47] E. Imre, S. Fityus, The use of the grading entropy as a measure of the soil texture maturity, ce/papers 2 (2–3) (2018) 639–644, doi:10.1002/cepa.742.

[48] S. Feng, P.J. Vardanega, E. Ibraim, Comparison of prediction models for the permeability of granular materials using a database, in: S. Hemeda, M. Bouassida (Eds.), Contemporary Issues in Soil Mechanics, Springer, Cham, Switzerland, 2019, pp. 1–13, doi:10.1007/978-3-030-01941-9_1.

[49] J. Lőrincz, Relationship between grading entropy and dry bulk density of granular soils, Period. Polytech. Civ. Eng. 34 (3) (1990) 255–265.

[50] M.A. James, The Grading Entropy and Permeability of Road Surfaces, University of Bristol, Bristol, UK, 2015 Research project report.

[51] L.A. Cooley Jr., E.R. Brown, S. Maghsoodloo, Development of Critical Field Permeability and Pavement Density Values for Coarse Graded Superpave Pavements, Auburn University, National Centre for Asphalt Technology, Auburn, AL, USA, 2001 Report no. 01-03.

[52] R.L. Schmitt, S. Owusu-Ababio, J.A. Crovetti, A.L. Cooley, Development of In-Place Permeability Criteria for HMA Pavement in Wisconsin, Wisconsin Highway Research Program, Madison, WI, USA, 2007 Report no. WHRP 06-15.

[53] R.B. Mallick, L.A. Cooley, M.R. Teto, R.L. Bradbury, D. Peabody, An Evaluation of Factors Affecting Permeability of Superpave Designed Pavements, National Centre for Asphalt Technology, Auburn University, Auburn, AL, USA, 2003 Report no. 03-02.

[54] A.K. Gogula, M. Hossain, P.E. Stefan, A. Romanoschi, A Study of Factors Affecting the Permeability of Superpave Mixes in Kansas, Kansas Department of Transportation, 2004 Technical Report, *KSU-00-02 KS, USA*.

[55] B. Choubane, G.C. Page, J.A. Musselman, Investigation of Water Permeability of Coarse Graded Superpave Pavements, Florida State Materials Office, FL, USA, 1997, pp. 97–416. Technical Report.

[56] J.S. Chen, K.Y. Lin, S.Y. Young, Effects of crack width and permeability on moisture-induced damage of pavements, J. Mater. Civ. Eng. 16 (3) (2004) 276–282, doi:10.1061/(asce)0899-1561(2004)16:3(276).

[57] V. Ranieri, J.J. Sansalone, S. Shuler, Relationships among gradation curve, Clogging Resist. Pore-Based Indices Porous Asph. Mix. Road Mater. Pavement Des. 11 (sup1) (2010) 507–525, doi:10.1080/14680629.2010.9690344.

[58] S. Takahashi, M.N. Partl, Improvement of mix design for porous asphalt, Road Mater. Pavement Des. 2 (3) (2001) 283–296, doi:10.1080/14680629.2001.9689904.

[59] L. Zhang, G. Ong, T. Fwa, Influences of pore size on the permeability and skid resistance of porous pavement, sustainability, eco-efficiency, and conservation in transportation infrastructure asset management, in: Proceedings of the 3rd International Conference on Transportation Infrastructure, CRC Press, 2014, pp. 621–632.

[60] Y. Jang, D. Kim, S. Mun, B. Jang, Proposal for the estimation of the hydraulic conductivity of porous asphalt concrete pavement using regression analysis, J. Korean Soc. Road Eng. 15 (3) (2013) 45–52, doi:10.7855/ijhe.2013.15.3.045.

[61] K. Kanitpong, H.U. Bahia, C.H. Benson, X. Wang, Measuring and predicting hydraulic conductivity (permeability) of compacted asphalt mixtures in the laboratory, in: Paper Presented at: 82nd Annu. Meet. Transp. Res. Board, Washington, DC, 2003.

[62] A. Setyawan, Design and properties of hot mixture porous asphalt for semi-flexible pavement applications, Media Tek. Sipil 36 (2005) 41–45.

[63] M.M. Sprinkel, A.K. Apeagyei, Evaluation of the installation and initial condition of thermoplastic polymer-modifed asphalt overlays on bridge decks, in: TRB 93rd Annual Meeting Compendium of Papers, 2014.

[64] B.J. Putman, Evaluation of Open-Graded Friction Courses: Construction, Maintenance, and Performance, US Department of Transportation Federal Highway Administration, South Carolina, USA, 2012 (Report No. FHWA-SC-12-04), Technical report https://rosap.ntl.bts.gov/view/dot/25181/dot_25181_DS1.pdf (accessed 24/09/2020).

[65] B. Choubane, G.C. Page, J.A. Musselman, Investigation of water permeability of coarse graded superpave pavements, J. Assoc. Asph. Paving Technol. 67 (1998) 254–276.
[66] S. Bhattacharjee, R.B. Mallick, An alternative approach for the determination of bulk specific gravity and permeability of hot mix asphalt (HMA), Int. J. Pavement Eng. 3 (3) (2002) 143–152, doi:10.1080/1029843021000067782.
[67] E.R. Brown, M.R. Hainin, A. Cooley, G. Hurley, Relationships of HMA in-place air voids, lift thickness, and permeability. volume one, NCHRP Web Document 68 (2020) https://onlinepubs.trb.org/onlinepubs/nchrp/nchrp_w68v1.pdf. 2004 (accessed 20 September.
[68] E.R. Brown, M.R. Hainin, A. Cooley, G. Hurley, Relationships of HMA in-place air voids, lift thickness, and permeability. volume two, NCHRP Web Document 68 (2020) https://onlinepubs.trb.org/onlinepubs/nchrp/nchrp_w68v2.pdf. 2004 (accessed 20 September.
[69] E.R. Brown, M.R. Hainin, A. Cooley, G. Hurley, Relationships of HMA in-place air voids, lift thickness, and permeability. volume three, NCHRP Web Document 68 (2020) https://onlinepubs.trb.org/onlinepubs/nchrp/nchrp_w68v3.pdf. 2004 (accessed 20 September.
[70] E.R. Brown, M.R. Hainin, A. Cooley, G. Hurley, Relationships of HMA in-place air voids, lift thickness, and permeability. volume four, NCHRP Web Document 68 (2004) https://onlinepubs.trb.org/onlinepubs/nchrp/nchrp_w68v4.pdf. (accessed 20 September 2020).
[71] J.E. Haddock, M. Prather, Investigation of permeability on Indiana SR-38, J. Perform. Constr. Facil. 18 (3) (2004) 136–141, doi:10.1061/(asce)0887-3828(2004)18:3(136).
[72] J. Norambuena-Contreras, E. Asanza Izquierdo, D. Castro-Fresno, M.N. Partl, G. Á, A new model on the hydraulic conductivity of asphalt mixtures, ISSN Int. J. Pavement Res. Technol. Int. J. Pavement Res. Technol. 6 (5) (2013) 488–495, doi:10.6135/ijprt.org.tw/2013.6(5).488.
[73] R.E. Pease, J.C. Stormont, J. Hines, D. O'Dowd, Hydraulic properties of asphalt concrete, Geotech. Test. J. 33 (6) (2010) 445–452, doi:10.1520/GTJ102644.
[74] Y.Y. Yan, J.P.J.P. Zaniewski, D. Hernando, Development of a predictive model to estimate permeability of dense-graded asphalt mixture based on volumetrics, Constr. Build. Mater. 126 (2016) 426–433, doi:10.1016/j.conbuildmat.2016.09.071.
[75] C. Hewitt, A study of asphalt permeability, BE(Hons) thesis, University of Central Queensland, Rockhampton, QLD, Australia, 1991.
[76] G. Maupin, Asphalt permeability testing in virginia, Transp. Res. Rec. J. Transp. Res. Board 1723 (2000) 83–91, doi:10.3141/1723-11.
[77] G. Maupin, Personal Communication, (2009).
[78] P.J. Vardanega, A. Nataatmadja, T. Waters, J. Ramanujam, A study of asphalt permeability: empirical permeability models, in: Proceedings of the 23rd ARRB Conference: Research - Partnering with Practitioners, ARRB Group Ltd, Melbourne, VIC, Australia, 2008.
[79] K. Kanitpong, C. Benson, H. Bahia, Hydraulic conductivity (permeability) of laboratory-compacted asphalt mixtures, Transp. Res. Rec. J. Transp. Res. Board 1767 (2001) 25–32, doi:10.3141/1767-04.
[80] F. H. Kulhawy, P. W. Mayne, Manual on estimating soil properties for foundation design, EL-6800 Research Project 1493-6, Final Report, (1990).
[81] G. Piñeiro, S. Perelman, J.P. Guerschman, J.M. Paruelo, How to evaluate models: Observed vs. predicted or predicted vs. observed? Ecol. Modell. 216 (3–4) (2008) 316–322, doi:10.1016/j.ecolmodel.2008.05.006.
[82] J.P. Stevens, Outliers and influential data points in regression analysis, Psychol. Bull. 95 (2) (1984) 334–344, doi:10.1037/0033-2909.95.2.334.
[83] G.C.J. Fernandez, Residual analysis and data transformations: important tools in statistical analysis, HortScience 27 (4) (1992) 297–300, doi:10.21273/HORTSCI.27.4.297.
[84] P.F. Velleman, R.E. Welsch, Efficient computing of regression diagnostics, Am. Stat. 35 (4) (1981) 234–242, doi:10.2307/2683296.
[85] T.J. Waters, A Study of the Infiltration Properties of Asphalt Road Materials, MAppSc thesis, Queensland University of Technology, Brisbane, QLD, Australia, 1990.
[86] J Ching, M Arroyo, J Chen, et al., Transformation models and multivariate soil databases, Joint TC205/TC304 Working Group on 'Discussion of Statistical/Reliability Methods for Eurocodes' (ISSMGE (International Society for Soil Mechanics and Geotechnical Engineering, 2017, pp. 1–19. (ed.)). ISSMGE, London, UK.
[87] M.K. Nivedya, R.B. Mallick, Artificial neural network-based prediction of field permeability of hot mix asphalt pavement layers, Int. J. Pavement Eng. 21 (9) (2020) 1057–1068, doi:10.1080/10298436.2018.1519189.
[88] ASTM International, D2487-17 Standard Practice for Classification of Soils for Engineering Purposes (Unified Soil Classification System), ASTM International, West Conshohocken, 2017. doi:10.1520/D2487-17E01.